Kotani, M. (1961) *Suppl. Prog. Theor. Phys. No. 17*, 4.

Marchon, J.-C., Mashiko, T., & Reed, C. A. (1982) in *Electron Transport and Oxygen Utilization* (Ho, C., Eaton, W. A., Collman, J. P., Gibson, Q. H., Leigh, J. S., Margoliash, E., Moffat, J. K., & Schiedt, W. R., Eds.) p 67, Elsevier Biomedical Press, New York.

Margalit, R., & Schejter, A. (1973) *Eur. J. Biochem. 32*, 494.

Ozols, J., & Strittmatter, P. (1969) *J. Biol. Chem. 244*, 6611.

Palmer, G. (1978) in *The Porphyrins* (Dolphin, D., Ed.) Vol. IV, Part B, p 313, Academic Press, New York.

Salmeen, I., & Palmer, G. (1968) *J. Chem. Phys. 48*, 2049.

Schejter, A., & Aviram, I. (1970) *J. Biol. Chem. 245*, 1552.

Schejter, A., Aviram, I., & Goldkorn, T. (1982) in *Electron Transport and Oxygen Utilization* (Ho, C., Eaton, W. A., Collman, J. P., Gibson, Q. H., Leigh, J. S., Margoliash, E., Moffat, J. K., & Scheidt, W. R., Eds.) p 95, Elsevier

Biomedical Press, New York.

Stephens, P. J., Sutherland, J. C., Cheng, J. C., & Eaton, W. A. (1976) in *The Excited States of Biological Molecules* (Birks, J. B., Ed.) p 434, Wiley, New York.

Tanford, C. (1961) *Physical Chemistry of Macromolecules*, Wiley, New York.

Taylor, C. P. S. (1977) *Biochim. Biophys. Acta 491*, 137.

Weissbluth, M. (1974) *Hemoglobin*, Springer-Verlag, New York.

Wüthrich, K. (1969) *Proc. Natl. Acad. Sci. U.S.A. 63*, 1071.

Wüthrich, K., Aviram, I., & Schejter, A. (1971) *Biochim. Biophys. Acta 253*, 98.

Yonetani, T., Iizuka, T., & Waterman, J. (1971) *J. Biol. Chem. 246*, 7683.

Zerner, M., Gouterman, M., & Kobayashi, M. (1966) *Theor. Chim. Acta 6*, 363.

Resonance Raman Spectra of Blue Copper Proteins: Assignments from Normal Mode Calculations and Copper-63/Copper-65 and H₂O/D₂O Shifts for Stellacyanin and Laccase[†]

Lisa Nestor, James A. Larrabee, Geoffrey Woolery, Bengt Reinhammar, and Thomas G. Spiro*

ABSTRACT: Resonance Raman (RR) spectra are reported for azurin, stellacyanin, and both tree and fungal laccase; effects of type 2 Cu removal on the laccase RR spectra are noted. Normal coordinate calculations are carried out on hypothetical Cu complexes with structures related to the known active-site structure of plastocyanin and azurin by using force constants transferred from model complexes. Among the Cu–ligand stretching coordinates, only the Cu–S(Cys) stretch contributes significantly to modes in the 400-cm⁻¹ region, where the strongest RR bands are found; Cu–N(His) stretching modes are expected in the 230–310-cm⁻¹ range. Stellacyanin and tree laccase have been reconstituted with ^{63}Cu and ^{65}Cu, and with D_2O, to assess the Cu and imidazole motions in the RR modes. A 2-cm⁻¹ D_2O/H_2O shift identifies the 273-cm⁻¹ stellacyanin RR band as a Cu–N(His) mode; the extent of the shift suggests that the C2, as well as N3 imidazole, proton was replaced by D. Much smaller D_2O/H_2O shifts are seen for the strong stellacyanin or laccase bands. The two strong RR bands of stellacyanin, 347 and 385 cm⁻¹, show 1.8- and 1.5-cm⁻¹ $^{63}Cu/^{65}Cu$ isotope shifts; the combined shift is that calculated for the Cu–S(Cys) stretch. It is suggested that the pair of bands arises from strong coupling between the Cu–S stretching and S–C–C bending coordinates of the bound cysteine. The average frequency is ~30 cm⁻¹ lower than the average frequencies of the strong bands in laccase, azurin, and plastocyanin, consistent with the longer extended X-ray absorption fine structure derived Cu–S distance in stellacyanin (2.19 Å) than in plastocyanin or azurin (2.13 Å). The laccase $^{63}Cu/$ ^{65}Cu shifts, however, 0.5 cm⁻¹ or less for the strong bands at 381, 405, and 420 cm⁻¹, are much lower than those for stellacyanin and additional couplings are implicated. A variety of angle-bending modes of the coordinated ligands are expected in the 300–500-cm⁻¹ region, but it is difficult to account for resonance enhancement for most of them. It is suggested that torsional motions about the cysteine S–C bond might contribute significantly to the resonance-enhanced modes.

The "blue" or type 1 site of copper proteins has long attracted a great deal of interest, because of its unusual spectroscopic properties (Malkin & Malmström, 1970; Fee, 1975; Gray & Solomon, 1981). In the past few years, the molecular and electronic structure of this site has come sharply into focus thanks to the application of a battery of physical methods, including absorption and circular dichroism (CD) spectroscopy (McMillen et al., 1974a,b; Solomon et al., 1976a,b), nuclear magnetic resonance (NMR) spectroscopy (Markley et al., 1975; Hill et al., 1976; Ugerbil et al., 1977), electron paramagnetic resonance (EPR) spectroscopy (Vanngard, 1972),

spin-echo EPR spectroscopy (Mims & Peisach, 1978, 1979), electron nuclear double resonance (ENDOR) spectroscopy (Roberts et al., 1980), X-ray crystallography [Colman et al., 1978; Adman et al., 1978; Freeman, 1980 (atomic coordinates in Brookhaven Protein Data Banks); Adman & Jensen, 1981], extended X-ray absorption fine structure (EXAFS) (Tullius et al., 1978; Peisach et al., 1982), and, recently, single-crystal absorption and EPR spectroscopy (Penfield et al., 1981). The X-ray crystal structure of oxidized plastocyanin [Freeman, 1980 (atomic coordinates in Brookhaven Protein Data Banks); Figure 1] and azurin (Adman et al., 1978) shows the copper ion to be coordinated to a cysteine sulfur and two hystidyl imidazole ligands, and also to a distant (2.9 Å) methionine sulfur atom, in a highly distorted tetrahedral complex. Stellacyanin has similar electronic properties but lacks methionine. The EXAFS analysis (Peisach et al., 1982) confirms the presence of two close N ligands and a close S ligand, with
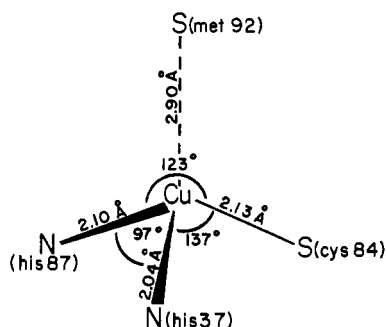
FIGURE 1: Active-site structure of poplar plastocyanin (Freeman, 1980).

distances differing only slightly from azurin (Tullius et al., 1978), and a probable distant ligand, of uncertain character.

Before this structural information became available, it had been established that laser excitation in the blue-site absorption band produces a resonance Raman (RR) spectrum with strong bands near 400 cm^{-1} and a number of weaker bands (Siiman et al., 1974, 1976; Miskowski et al., 1975). The strong bands were assumed to arise from Cu^{II}–ligand stretching modes, and since the $\sim$400-cm^{-1} region is characteristic of aliphatic nitrogen or oxygen ligands (Nakamoto, 1978), coordination by side-chain amine, hydroxyl, or carboxylate groups was indicated.

Understanding the RR spectrum remains an outstanding problem in characterizing the blue site. While Cu–S(Cys) stretching might contribute to the dominant $\sim$400-cm^{-1} RR bands, in view of the short Cu–S(Cys) bond distances that have been determined [Freeman, 1980 (atomic coordinates in Brookhaven Protein Data Banks); Tullius et al., 1978; Peisach et al., 1982], it seems unlikely that the Cu–N(His) stretches are much higher than their usual value of $\sim$250 cm^{-1} (Nakamoto, 1978), suggestions to the contrary (Siiman & Carey, 1976; Thamann et al., 1982) notwithstanding, since the Cu–N(His) distances are quite normal. This point has been made by Woodruff and co-workers (Woodruff et al., 1983a,b,c), who have reported highly resolved blue-site RR spectra at low temperature and have suggested that the wealth of bands observed must reflect contributions from deformation modes of the coordinated ligands. In the present work, the problem of band assignments is addressed with the aid of normal coordinate calculations and of isotope shifts induced by reconstituting two blue proteins, stellacyanin and laccase, with ^{63}Cu and ^{65}Cu, and in D$_2$O and H$_2$O. It is concluded that only Cu–S(Cys), among the Cu–ligand stretching coordinates, contributes to the $\sim$400-cm^{-1} modes and that it couples strongly with internal ligand deformation coordinates in giving rise to the observed bands. The Cu–N(His) stretching coordinates contribute mainly to the 270-cm^{-1} band. In addition, the type 1 RR spectrum of fungal laccase B is reported [during the preparation of the manuscript, the spectrum of fungal laccase A was reported independently by Blair et al. (1983)] as are the effects of anion binding at the type 2 Cu^{II} and of type 2 Cu^{II} removal.

Experimental Procedures

Rhus vernicifera laccase and stellacyanin were prepared (Reinhammar, 1970) from Chinese or Japanese lacquer acetone powder (Saito and Co., Ltd). The final chromatographic purification was repeated until A_{280}/A_{614} = 15.7–15.2 for laccase and A_{280}/A_{604} = 6.0–5.6 for stellacyanin (95–100% purity). A 200-g aliquot of acetone powder gave $\sim$2.7 g of laccase and $\sim$0.25 g of stellacyanin. The physical properties of protein samples from the Chinese or Japanese lacquer tree

were the same. Fungal laccase B was prepared from *Polyporous versicolor* by the method of Fahracus & Reinhammar (1967). Highly purified azurin from *Pseudomonas aeruginosa* (A_{625}/A_{289} = 0.59, electrophoretically homogeneous) was obtained from the Microbiological Research Establishment (Proton-Down Salisbury, SP4-0JG Wlts, U.K.). Protein concentrations were adjusted via ultrafiltration and monitored spectrophotometrically.

Apostellacyanin (Morpurgo et al., 1972) and apolaccase (Larrabee & Spiro, 1979) were prepared and reconstituted by anaerobic incubation with cuprous chloride in excess sodium chloride (Hauenstein et al., 1978) for 4–5 days, followed by exhaustive dialysis against Tris [tris(hydroxymethyl)aminomethane] buffer (25 mM, pH 7.4, for laccase and 50 mM, pH 8.2, for stellacyanin). Isotopic CuCl was prepared by dissolution in HCl of ^{63}Cu$_2$O and ^{65}Cu$_2$O, prepared (Parker, 1964) from the corresponding curpic oxides (99.9% ^{63}Cu and 99.7% ^{65}Cu, Oak Ridge National Laboratories). Reconstitution with natural abundance CuCl was also carried out in D$_2$O; the same D$_2$O RR shifts were obtained when native protein was dialyzed exhaustively against D$_2$O buffer at 4 °C.

Anion binding of tree laccase was studied by adding NaN$_3$ or KSCN to a concentration of 2.1 and 0.2 M, respectively, in the protein solution. Removal of type 2 copper (Graziani et al., 1976) from tree and fungal laccase was carried out as described by Reinhammar & Oda (1979) and by Malkin et al. (1969), respectively. The product was checked by EPR and absorption spectroscopies.

Raman spectra were excited with the 647.1-nm line of the Kr$^+$ laser or with an Ar$^+$-pumped dye laser (Rhodamine 6G) and were recorded with a Spex 1401 double monochromator equipped with a cooled RCA C31304A photomultiplier and photon-counting electronics. The data were collected digitally with a DEC MINC computer. A spinning sample cell was used for ordinary room-temperature spectra. Difference Raman spectra were obtained with a split spinning cell or with a 10-mm NMR tube fitted with a Teflon divider and used in a back-scattering arrangement. The triggering system employed two Texas Instruments L139 JR emitter/receivers, which alternately sensed reflection tape on each half of the divided cell. The two spectra were collected simultaneously on a dual-channel ORTEC Model 9315 photon counter and were stored and subtracted with the MINC computer. The experimental technique used for the frozen solution spectra has been described elsewhere (Johnson & Czernuszewicz, 1983).

Results and Discussion

Spectral Characteristics. Figure 2 shows room-temperature RR spectra of azurin, stellacyanin, and tree laccase, obtained with 600-nm Rhodamine 6G dye laser excitation, at the center of the blue absorption bands. The spectra are characterized by two or three intense bands near 400 cm^{-1}, a band of moderate intensity at $\sim$270 cm^{-1}, and many weak bands from 100 to 500 cm^{-1}. Clusters of bands are observed near 800 cm^{-1}, which plausibly contain a superposition of overtones and combinations of the dominant $\sim$400-cm^{-1} bands, as illustrated in Figure 3, and, in addition, a distinct band at 750 cm^{-1}, which Ferris et al. (1979) assigned to C–S stretching of the cysteine ligand. The C–S stretching frequency in thiols is found in the 650–710-cm^{-1} range (Scott & El-Sabban, 1969), and an increase to 750 cm^{-1} might arise from coupling with the Cu–S stretch of the thiolate ligand.

Siiman et al. (1974) reported bands at 1249 and 1650 cm^{-1} in blue protein RR spectra, assignable to amide I and III modes of the peptide backbone. This was taken as evidence
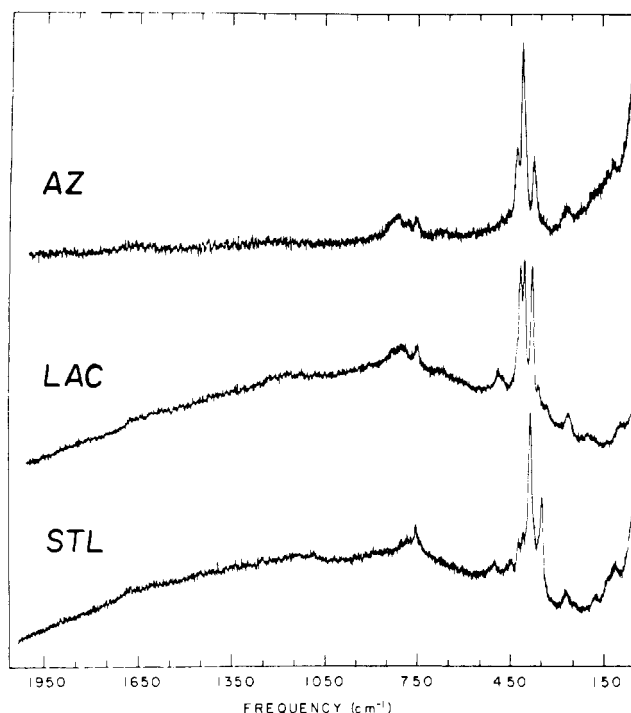
FIGURE 2: Raman spectra of copper proteins in resonance with the blue absorption band. (AZ) 0.92 mM *P. aerugnosa* azurin in 0.05 M sodium acetate sulfer, pH 6.0; 596.8-nm laser excitation (50 mW); 8-cm^{-1} spectral slit width. (LAC) 1 mM *R. vernicifera* laccase in 0.05 M potassium phosphate buffer, pH 6.0; 605.5-nm laser excitation (200 mW); 5-cm^{-1} spectral slit width. (STL) 1 mM *R. vernicifera* stellacyanin in 0.05 M potassium phosphate buffer, pH 6.0; 605.5-nm laser excitation (200 mW); 5-cm^{-1} spectral slit width. The spectra were recorded at 0.5-cm^{-1} increments with photon counting for 2 s.

for peptide–N coordination to Cu^{II} although the subsequent crystal structures of plastocyanin and azurin ruled this out. Our RR spectra (Figure 2) did not show these features, but they did appear when the excitation wavelength was tuned off-resonance (570 nm). (The wavelengths used by Siiman et al., 647.1 and 568.2 nm, were likewise somewhat off-resonance.) We conclude that the 1240- and 1650-cm^{-1} bands are nonresonance protein modes.

The weak features in the RR spectra are brought out more clearly in low-temperature (77 K) frozen solution spectra, as illustrated for laccase (in Figure 4). The bands are sharpened considerably due to the cooling out of hot bands (Johnson & Cernuscewicz, 1983). Woodruff et al. (1983a,b) have reported still more detailed spectra of azurin and plastocyanin obtained at 12 K. Table I summarizes the observed frequencies.

With 4579-Å excitation, the dominant stellacyanin RR bands at ~350 cm^{-1} were still seen, although weakly, and scanning to higher frequencies revealed only a rising background, due to a luminescence process of unknown origin. This wavelength is in a moderately strong ($\epsilon \sim 1000$ M cm^{-1}) absorption band ($\lambda_{max} = 450$ nm) that has been suggested (Solomon et al., 1980) to be due to imidazole $\rightarrow$ Cu^{II} charge transfer, the unusually low energy for such a transition (Fawcett et al., 1980) being associated with the nontetragonal character of the Cu^{II} site. Excitation in such a band is expected (Walters & Spiro, 1983) to provide modest enhancement of imidazole ring modes. These were not observed in our 4579-Å RR spectrum, but they may have been obscured by the high background.

Figure 5 compares the 647.1-nm RR spectrum of fungal laccase B [which agrees with that recently reported for fungal laccase A by Blair et al. (1983)] with that of tree laccase and also shows the effect of removing type 2 Cu^{II}. Binding of the
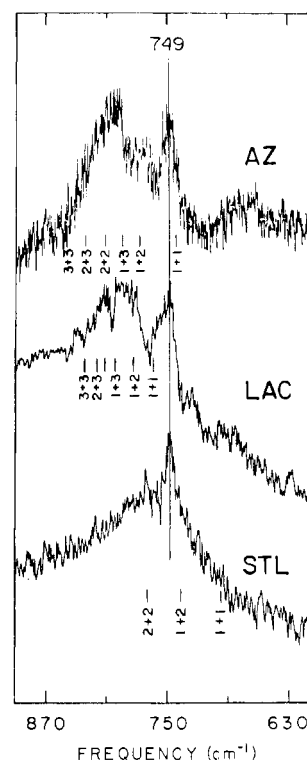

FIGURE 3: Expanded resonance Raman spectra of blue copper proteins azurin (AZ), tree laccase (LAC), and stellacyanin (STL) in the 600–900-cm^{-1} region. Solution and excitation conditions as in Figure 1. Overtone and combination tone positions for the prominent RR bands are indicated by the short lines: (1–3) 371, 406, and 426 cm^{-1} for AZ and 381, 405, and 419 cm^{-1} for LAC; (1 and 2) 348 and 385 cm^{-1} for STL. The common band, at 749 cm^{-1}, is assigned to C–S–(Cys) stretching.

Table I: Observed Resonance Raman Bands (cm^{-1}) for Laccase and Stellacyanin in Frozen Solution (~77 K) and for Azurin at Room Temperature

~77 K laccase (ΔD) [ΔCu][a]	~77 K stellacyanin (ΔD) [ΔCu][a]	RT azurin
99	118	113
202	177	268
265	243	371
333	273	406
346	334 (sh)	426
361	347 (1.8)	456 (sh)
381 (0.8) [0.5]	~359 (sh) (~2–3)	748
405 (~0.5) [0.5]	~374 (sh) (~2–3)	775
420	385 [0.6]	803
~426	405 [1.5]	822 (sh)
445	422	
470	444	
490	663	
750	734	
768	746	
793	769	
806		
825		

[a] Numbers in parentheses and brackets give isotope downshifts upon substituting D$_2$O for H$_2$O (ΔD) or ^{65}Cu for ^{63}Cu [ΔCu], respectively.

anions N$_3^-$ and SCN$^-$ to the type 2 site (Reinhammar & Malmström, 1981) has no effect at all on the type 1 RR spectrum of tree laccase, nor does F$^-$ binding (Blair et al., 1983). This is in contrast to the report by Tosi et al. (1975) that anion binding does perturb the RR spectrum of ceruloplasmin in a manner suggesting a structural change at one of the two type 1 sites of that protein. Removal of the type 2 Cu^{II} lowers the intensity of one of the tree laccase bands, 381
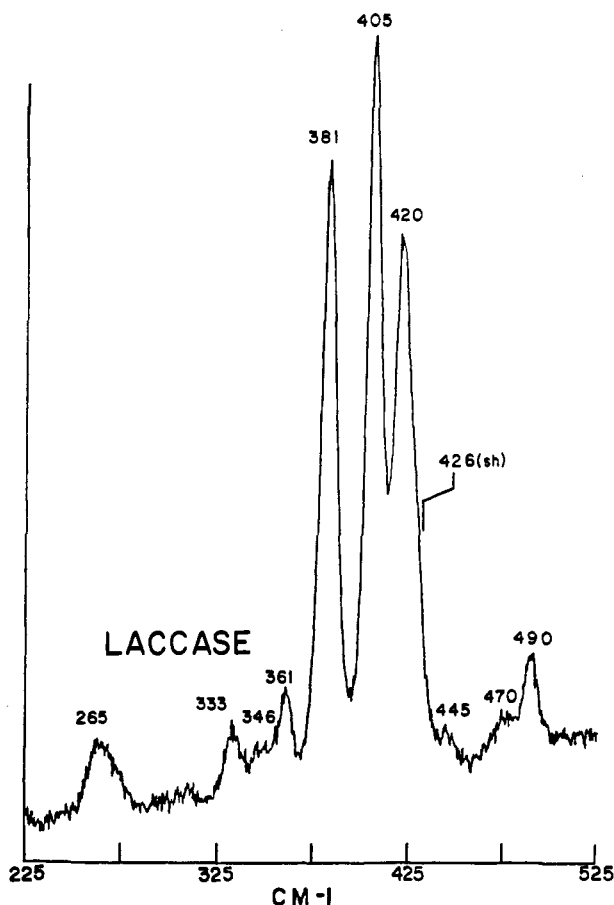
FIGURE 4: Frozen solution spectrum of ~2 mM *Rhus vernicifera* laccase in 50 mM pH 7.4 Tris buffer with 647.1-nm laser excitation (125 mW) and a 5-cm⁻¹ spectral slit width. Nine spectra were added together, each recorded at 0.5-cm⁻¹ increments with photon counting for 2 s.

cm⁻¹. This is in agreement with the recent report of LuBien et al. (1981), who attributed the spectral perturbation to reduction of the type 3 site (as determined by X-ray absorption spectroscopy), although the extent of reduction appears to be preparation dependent (Reinhammar, 1983). The intensity loss is restored upon treatment of the protein with H_2O_2. The fungal laccase spectrum appears to correlate band for band with the tree laccase spectrum, but all the frequencies are slightly higher (2–8 cm⁻¹). The bands at 407 and 387 cm⁻¹ are much lower in relative intensity than the corresponding bands in tree laccase. Removal of type 2 Cu^{II} from the fungal laccase spectrum produces a further lowering of both the 407- and the 387-cm⁻¹ band intensities.

Isotope Shifts. In order to determine the contribution of Cu–ligand stretching to the observed RR bands, both stellacyanin and tree laccase were reconstituted with the isotopes ^{63}Cu and ^{65}Cu. In addition, they were reconstituted with natural abundance Cu but with D_2O instead of H_2O, the intention being to identify the contributions of Cu–N(His) stretching (Larrabee & Spiro, 1980). The N3 proton of imidazole exchanges on contact with D_2O, and the C2 proton exchanges more slowly (Markley, 1975; Markley et al., 1975). Under reconstituting conditions, both protons can be expected to exchange, and the extent of the observed RR frequency shifts seems to bear this out (vide infra).

Figure 6 shows room-temperature RR difference spectra for stellacyanin. The ^{63}Cu–^{65}Cu difference spectrum shows clear derivative lines centered at the 347- and 385-cm⁻¹ band maxima. Frequency shifts were calculated (Shelnutt et al., 1979) from the peak and derivative amplitude ratios to be 1.8
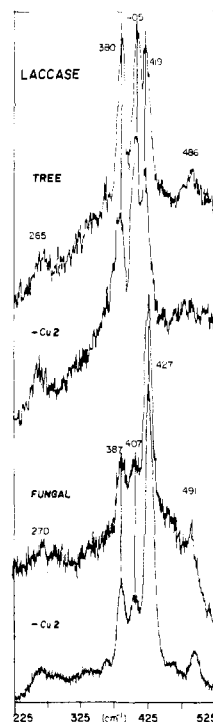

FIGURE 5: Raman spectra for tree and fungal laccase, showing the effect to type 2 Cu removal (-Cu2). All solutions were 1 mM in protein, in 0.05 M KH_2PO_4, pH 6.0. 647.1-nm laser excitation (200 mW); 10-cm⁻¹ spectral slit width; 0.5-cm⁻¹ increments with 2-s photon counting.
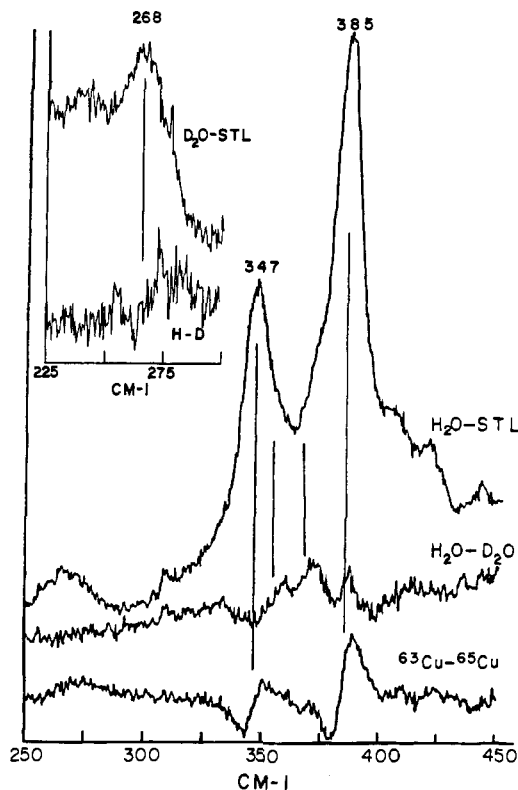

FIGURE 6: H_2O – D_2O and ^{63}Cu – ^{65}Cu difference spectra for 1 mM *R. vernicifera* stellacyanin in 25 mM pH 8.2 Tris buffer with 647.1-nm laser excitation (125 mW) and an 8-cm⁻¹ spectral slit width. The H_2O – D_2O spectrum was taken in a divided NMR tube with photon counting for 20 s at 0.5-cm⁻¹ increments. The ^{63}Cu – ^{65}Cu spectrum was taken in a split spinning cell under the same conditions. (Insert) H_2O – D_2O stellacyanin spectrum of the 260-cm⁻¹ region with photon counting for 90 s.

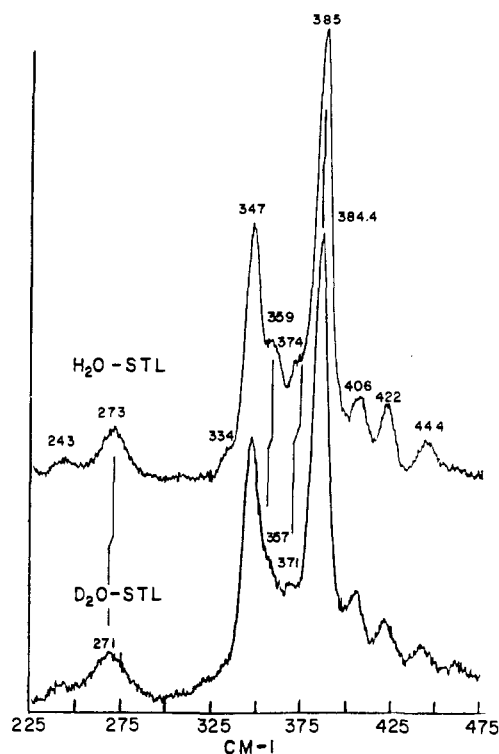and 1.5 cm⁻¹, respectively. Thus, these modes involve substantial motions of the Cu atom. The 268-cm⁻¹ band, however,

FIGURE 7: Frozen solution spectra for $\sim$2 mM H_2O – stellacyanin and D_2O – stellacyanin with solution and excitation conditions as in Figure 6. Nine spectra were added together, each recorded at 0.5-cm^{-1} increments with photon counting for 2 s.

FIGURE 8: H_2O – D_2O and ^{63}Cu – ^{65}Cu difference spectra for $\sim$1 mM laccase from *R. vernicifera* with solution and excitation conditions as in Figure 4. The sampling conditions were as in Figure 6, with photon counting at 0.5-cm^{-1} increments for 30 s.

does not show an inflection in the difference spectrum but only a weak maximum, reflecting a slight intensity change but no appreciable frequency shift.

The H_2O–D_2O difference spectrum is more complex. A derivative line shape is seen for the 385 cm^{-1} band, corresponding to a 0.8-cm^{-1} shift, but the 347-cm^{-1} band shows a minimum, reflecting an intensity change without a frequency shift. There are, in addition, inflections associated with shoulders between the two strong bands, at 359 and 374 cm^{-1}. Finally, the 268-cm^{-1} band also gives an inflection, as shown in the inset. This band is asymmetric and contains more than one component, making evaluation of the frequency shift uncertain. At 77 K (Figure 7), the band sharpens appreciably, and its center shifts to 273 cm^{-1}. A $\sim$2-cm^{-1} downshift in D_2O is now evident. The 359- and 374-cm^{-1} shoulders also sharpen at 77 K, and their D_2O downshifts are clearly seen.

Figure 8 shows RR difference spectra for tree laccase. The 381- and 405-cm^{-1} bands show ^{63}Cu–^{65}Cu derivative lines, corresponding to frequency shifts of 0.5 and 0.5 cm^{-1}. Significant Cu motion is implicated for these modes, although the shifts are only $\sim$$\frac{1}{3}$ of those seen for the 347- and 385-cm^{-1} stellacyanin bands. There also appears to be a slight inflection at the position of the 420-cm^{-1} band, but it is barely above the noise level, and the shift is certainly smaller than 0.5 cm^{-1}. The H_2O–D_2O difference spectrum likewise shows derivative line shape coincident with the 381- and 405-cm^{-1} bands, corresponding to 0.8- and $\sim$0.5-cm^{-1} shifts. No detectable shift is seen for the 420-cm^{-1} band. The 265-cm^{-1} band, which again contains more than one component, was too poorly defined to measure a reliable H_2O/D_2O shift.

Mode Assignments. (1) Metal–Ligand Modes. (a) Cu–S(Met) Stretching. In considering the vibrational frequencies to be expected of a blue Cu chromophore, we used the X-ray crystal structure (Freeman, 1980; atomic coordinates in Brookhaven Protein Data Banks) of plastocyanin (Figure 1) as the point of departure. Azurin is known to have a similar
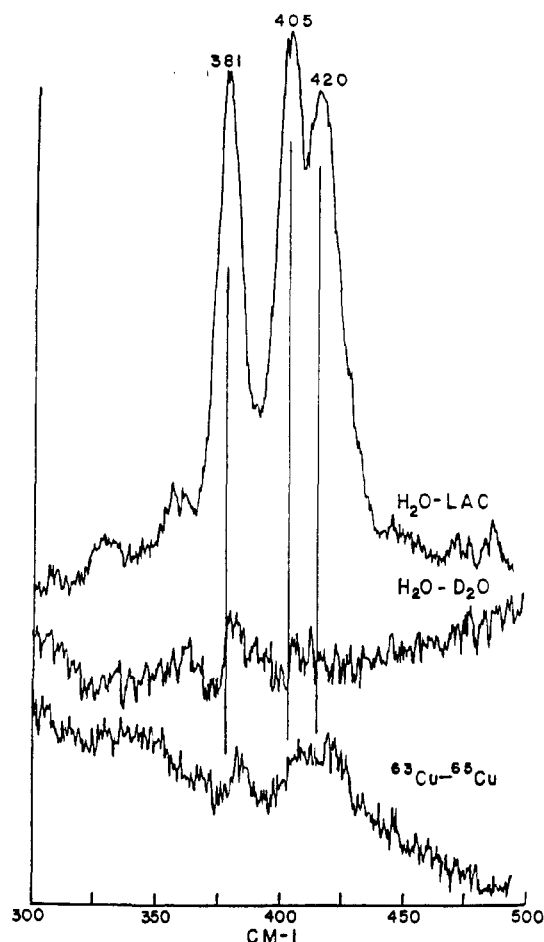
Cu coordination group (Adman & Jensen, 1981), and the similarity in electronic and EPR spectra of all blue sites makes it likely that they have similar structures. Methionine is not an invariant feature of the site, since stellacyanin has no methionine (Peisach et al., 1967). It has been suggested (Ferris et al., 1978) that a disulfide group replaces methionine in the stellacyanin Cu site.

Cu^{II}–thioether complexes show Cu–S stretching frequencies in the 250–280-cm^{-1} region, and it had been suggested (Ferris et al., 1978) that the $\sim$260-cm^{-1} RR band seen for all blue proteins might arise from Cu–S(Met) (or Cu–disulfide) stretching. However, the Cu^{II}–S(Met) distance in plastocyanin, 2.9 Å, is $\sim$0.6 Å longer than typical Cu^{II}–thioether bonds (Glick et al., 1976), and the stretching frequency should therefore be much lower. Moreover, Hodgson and co-workers (Scott et al., 1982) have been unable to find any evidence of a Cu–S(Met) interaction in the EXAFS spectrum of oriented plastocyanin crystals even when the X-ray polarization is aligned with the Cu–Met direction. They attributed this negative finding to a high Debye–Waller factor associated with uncorrelated motions of the Cu and S(Met) atoms, i.e., to the lack of a chemical bond. Moreover, the polarized absorption spectra of plastocyanin crystals (Penfield et al., 1981) have been interpreted without recourse to S(Met) → Cu^{II} charge-transfer contributions. The (isotropic) EXAFS spectrum of stellacyanin likewise shows no evidence of nearest-neighbor atoms beyond a single S and two N atoms (Peisach et al., 1982). Consequently, it seems unlikely that the RR spectrum of these species is detectably influenced by the Met (or disulfide) group. Woodruff et al. (1983b) have, however, at-

tributed bands at 287, 569, and 657 cm^{-1}, which appear in the 12 K RR spectrum of azurin, to Cu–S(Met) and two S–C-(Met) stretching modes and have suggested significant Cu–S(Met) bonding at low temperatures.

(b) *Cu–N(His) Stretching.* Cu^{II} imidazole complexes show Cu–ImH (ImH = imidazole) stretching vibrations in the 250-cm^{-1} region, although the Cu^{II}–N stretches of acyclic N ligands are much higher, ~400 cm^{-1} (Nakamoto, 1978). The depressed Cu–ImH frequency is attributable to strong coupling between the Cu–N stretching and C–N–C in-plane deformation coordinates, resulting in an effective ligand mass that is close to the mass of the entire ImH ring. This effect is illustrated in a related system, the bis(pyridine) complex of Fe^{II}–mesoporphyrin (Wright et al., 1979), for which the symmetric stretch of the *trans*-pyridine ligands is at the very low frequency of 179 cm^{-1}. This frequency was calculated to within 5 cm^{-1} by using a triatomic model with point ligands carrying the full pyridine mass and the same force constant that was obtained with a normal mode analysis that included all the pyridine atoms. The eigenvector of the 179-cm^{-1} mode showed all the pyridine atoms moving away from the Fe atom in concert, providing further justification for the point-mass approximation.

If any of the prominent ~400-cm^{-1} RR bands of blue proteins were assigned to Cu–ImH stretching, a roughly 2-fold increase in the usual Cu–ImH force constant would be implied, since the force constant scales with the square of the frequency. Yet, the Cu–ImH bond distances, as determined by crystallography or EXAFS, are within the normal range, 2.0 ± 0.1 Å. Recognizing that such large force constants are unreasonable, Thamann et al. (1982) used the mass of N (14) instead of ImH (68) in their recent point-ligand normal-mode calculations, in order to obtain a reasonable fit to the strong azurin RR bands. It is hard to see how this approximation can be justified, however. The effective ImH mass might be reduced if the Cu–N bond was tilted away from the plane of the ImH ring, thereby reducing the coupling with the in-plane ring deformation. A very large tilt, close to 90°, would be required to lower the mass to the vicinity of 14, however, and this is chemically unreasonable. In any event, the plastocyanin crystal structure shows the deviations of the Cu–N bonds from the ImH planes to be less than 10° (H. C. Freeman, private communication).

Measurable isotope shifts of Cu–ImH stretching modes are expected when the N3 proton of the bound imidazole is exchanged for deuterium. The 245-cm^{-1} Cu–ImH breathing mode of Cu(ImH)$_4^{2+}$ shifts down by 1.2 cm^{-1} when the complex is dissolved in D$_2$O and by 2.4 cm^{-1} when the C2 proton is also exchanged (Larrabee & Spiro, 1980). Increasing the ImH mass from 68 to 69 shifts the frequency of a hypothetical Cu–ImH diatomic oscillator by 0.9 cm^{-1} at 250 cm^{-1} and by 1.4 cm^{-1} at 400 cm^{-1}. The expected frequency shifts double if the C2 and the N3 protons are exchanged, as seems likely in the present study (vide infra). The H$_2$O/D$_2$O frequency shifts observed for stellacyanin and laccase, however, are less than 0.8 cm^{-1} for any of the intense ~400-cm^{-1} bands, but the shift is ~2 cm^{-1} for the 273-cm^{-1} band of stellacyanin (the shift of the analogous laccase band could not be determined). The latter band is therefore implicated as a Cu–ImH stretch, whereas the shifts of the ~400-cm^{-1} bands are too small for such an assignment.

(c) *Cu–S(Cys) Stretching.* Characteristic Cu–SR stretching frequencies are not well documented, but the spectrum of the Cu^{2+} complex of (α-mercaptopropionyl)glycine suggests assignment of $\nu_{Cu–SR}$ to a band at 303 cm^{-1} (Ferris et al., 1978).

The Cu–S(Cys) bond distance is 2.13 Å in plastocyanin (Freeman, 1980; atomic coordinates in Brookhaven Protein Data Banks) and azurin (Tullius et al., 1978) and is 0.1–0.2 Å shorter than expected for Cu^{II}–thiolate bonds (Tullius et al., 1978). The Cu–S(Cys) frequency is therefore expected to be unusually high. If the force constant scales with the distance according to Badger's rule (Herschbach & Laurie, 1961), then a 0.2-Å decrease in bond length is enough to raise the Cu–S stretching frequency from ~300 to ~400 cm^{-1}. Thus it is plausible that one of the prominent bands in the 400-cm^{-1} region of blue protein RR spectra is accountable to Cu–S(Cys) stretching. The short Cu–S distance in stellacyanin, 2.19 Å (Peisach et al., 1982), is 0.06 Å longer than that in plastocyanin and azurin, and this may account for the prominent stellacyanin RR bands, 347 and 385 cm^{-1}, being somewhat lower in frequency than those of other blue proteins.

(2) *Calculation of Metal–Ligand Frequencies.* In order to put these considerations of expected metal–ligand frequencies on a firmer basis, we carried out model normal-coordinate calculations on a hypothetical Cu–ligand with point-mass ligands (68 for the His ImH ring, 32 for the Cys and Met S atoms), having the geometry found for the Cu coordination group in oxidized plastocyanin (Figure 1). The aim was not to fit the observed protein spectra but rather to estimate what the Cu–ligand frequencies would be if the bonds were isolated from the rest of the protein.

A Urey–Bradley force field was chosen, because of the likely importance of nonbonded ligand–ligand forces (Shimanouchi et al., 1966). Model complexes of known structure and well-assigned vibrational frequencies were chosen, and their Urey–Bradley force constants were calculated. These were subsequently adjusted to the plastocyanin structure by using Badger's rule (Herschbach & Laurie, 1961) to scale the metal–ligand stretching constants, K, and an r^{-11} (r = interatomic distance) dependence to scale the nonbonded constants, F (Shimanouchi et al., 1966). The angle-bending constants, H, were scaled as the geometric mean of stretching constants of the bonds forming the angle. FeCl$_4^-$ (Avery et al., 1968) was chosen to model the Cu–S and S$\cdots$S interactions, since Cl$^-$ is isoelectronic with S^{2-} and the Fe–Cl distance, 2.19 Å (Zaslow & Rundle, 1961), is close to the Cu–S(Cys) distance. The Cu–ImH and ImH$\cdots$ImH interactions were modeled with Ni(ImH)$_6^{2+}$ (Goodgame et al., 1968), whose Ni–N bond distance, 2.13 Å (Santoro et al., 1969), is close to the Cu–N(His) distances. The S$\cdots$ImH nonbonded constant and the S–Cu–ImH bending constants were taken as the geometric mean of the extrapolated S$\cdots$S, ImH$\cdots$ImH and S–Cu–S, ImH–Cu–ImH pairs.

Table II gives the values of the adjusted force constants and calculated frequencies, isotope shifts, and potential energy distributions for three different model calculations. In model I, the structure parameters were those reported for the plastocyanin crystal structure (Freeman, 1980; atomic coordinates in Brookhaven Protein Data Banks). These include two different Cu–N distances, 2.10 and 2.04 Å, whereas the EXAFS-derived Cu–N distance is 1.95 Å (Tullius et al., 1978). While these differences are within the error limits of protein crystallography, they are large enough to have a significant effect on the vibrational frequencies. In model II, both Cu–N distances were set to 1.95 Å, with all other parameters held fixed, and the force constants readjusted accordingly. In model III, the Cu–S(Cys) distance, which is 2.13 Å from crystallographic and EXAFS determinations for plastocyanin and azurin, was lengthened to 2.19 Å, the EXAFS-derived value for stellacyanin (Peisach et al., 1982).

Table II: Normal Coordinate Calculations and Calculated Frequencies for Blue-Site Cu with Point-Mass Ligands in the Plastocyanin Geometry (Figure 1)

Urey-Bradley force constant[a]	mdyn/A		
	model I[b]	model II[c]	model III[d]
K_{Cu-Sm}	0.364	0.364	0.364
K_{Cu-Sc}	1.77	1.77	1.51
K_{Cu-N87}	1.20	1.76	1.76
K_{Cu-N37}	1.39	1.76	1.76
$H_{N37-Cu-N87}$	0.164	0.223	0.223
$H_{Sm-Cu-N87}$	0.029	0.036	0.036
$H_{Sc-Cu-N87}$	0.065	0.079	0.073
$H_{Sm-Cu-N37}$	0.032	0.036	0.036
$H_{Sc-Cu-N37}$	0.070	0.079	0.073
$H_{Sc-Cu-Sm}$	0.013	0.013	0.012
$F_{Sm-Cu-Sc}$	0.015	0.053	0.047
$F_{Sm-Cu-N37}$	0.029	0.037	0.037
$F_{Sm-Cu-N87}$	0.142	0.167	0.167
$F_{Sc-Cu-N87}$	0.052	0.077	0.064
$F_{Sc-Cu-N37}$	0.025	0.032	0.026
$F_{N87-Cu-N37}$	0.113	0.218	0.218

stretching modes			PED (%)[g]			bending modes
ν (cm^{-1})	ΔCu^e	ΔD^f	Cu-Sc	Cu-N	Cu-Sm	(cm^{-1})
Model I						
400.8	2.8	0.2	83	17		93.6
268.9	2.2	2.3	2	94		86.9
232.8	0.7	2.1	11	79		70.0
186.2	0.7			2	79	59.3
						43.3
Model II						
412.7	3.3	0.4	75	22		118.0
314.3	2.7	2.0		97		96.9
266.7	0.5	2.2	20	68		78.4
189.9	0.6				76	60.8
						48.8
Model III						
389.7	3.2	0.5	67	29		117.1
313.7	2.7	2.0		97		96.5
260.4	0.3	2.0	27	61		72.8
189.4	0.6	0.1			76	57.3
						48.6

[a] Sm = S of Met; Sc = S of Cys; N87 = N of His-87; N37 = N of His-37. [b] Plastocyanin crystal structure parameters: Cu-Sm = 2.90 A, Cu-Sc = 2.13 A, Cu-N87 = 2.10 A, Cu-N37 = 2.04 A; ∠Sm-Cu-Sc = 105°, ∠Sm-Cu-N = 100° C, ∠Sm-Cu-N37 = 83°, ∠Sc-Cu-N87 = 120°, ∠Sc-Cu-N37 = 139°, ∠N87-Cu-N37 = 97°. [c] Same as model I, except Cu-N87 = Cu-N37 = 1.95 A. [d] Same as model II, except Cu-Sc = 2.19 A. [e] ΔCu, ^{63}Cu/^{65}Cu isotope shift. [f] ΔD, shift on replacing two protons with deuterium on each ImH. [g] PED, potential energy distributions; % contribution from the force constants for stretching of the indicated bonds. The Cu-N entry is the sum of contributions for Cu-N87 and Cu-N37.

All of these calculations give a predominantly Cu–S(Cys) stretch at ∼400 cm^{-1}, a mainly Cu–S(Met) stretch at ∼175 cm^{-1}, and two Cu–N(His) stretches in the 230–310-cm^{-1} range. The Cu–S(Met) frequency is highly uncertain in view of the large interatomic distance found in plastocyanin and the possibility that there is no Cu–S(Met) bond in any meaningful sense. The remaining three Cu–ligand stretches are in the regions expected on the basis of the qualitative considerations discussed above. Of the two Cu–N(His) modes, the symmetric one lies lower in frequency, mixes significantly with the Cu–S(Cys) stretch, and has a small predicted ^{63}Cu/^{65}Cu isotope shift. Since it is the symmetric mode that is expected to be more strongly enhanced via Frank–Condon scattering, which is the dominant mechanism for resonance with allowed electronic transitions (Spiro & Stein, 1977), the ∼270-cm^{-1} RR
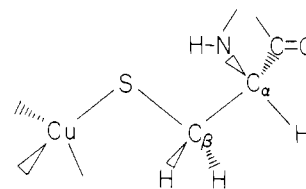

FIGURE 9: Diagram of the copper–cysteine fragment of the blue site.

band of blue proteins is reasonably assigned to this mode. The ∼2-cm^{-1} D_2O/H_2O shift observed for this band in stellacyanin is in good agreement with the calculated shift, which assumes a two unit mass change (i.e., deuteration at N3 and C2).

The Cu–S(Cys) stretch is calculated at ∼400 cm^{-1}, close to the frequency averages of the most intense bands of laccase (405 cm^{-1}), azurin (400 cm^{-1}), and plastocyanin (403 cm^{-1}; Woodruff et al., 1983). The 20-cm^{-1} calculated reduction upon lengthening the Cu–S(Cys) bond from 2.13 to 2.19 Å is not far from the difference between these averages and the average for stellacyanin (366 cm^{-1}). The calculated ^{63}Cu/^{65}Cu isotope shift, however, 2.8–3.3 cm^{-1}, is much larger than the observed shift of any single band of stellacyanin or laccase. The calculated shift is equal to the combined shifts of the stellacyanin 385- and 347-cm^{-1} bands. It is therefore reasonable to suppose that this pair of bands arises from strong coupling between the Cu–S(Cys) mode and another mode of similar energy. The likely nature of this coupling is discussed in the next section. The H_2O/D_2O shift of the 385-cm^{-1} stellacyanin band (0.8 cm^{-1}) is somewhat greater than calculated for the Cu–S(Cys) stretch; the calculated value increases with the extent of mixing of Cu–N(His) stretching (see model I in Table II), and the larger observed shift suggests somewhat greater mixing than calculated.

Laccase shows smaller H_2O/D_2O shifts for its prominent bands, at 381, 405, and 420 cm^{-1}, and the combined ^{63}Cu/^{65}Cu shifts for these bands, <1.5 cm^{-1}, is less than half of the calculated shift of the Cu–S(Cys) stretch. Thus the pattern of vibrational couplings must be appreciably different for laccase than for stellacyanin.

(3) Ligand Modes. As Woodruff et al. (1983a,b,c) have pointed out, there are far too many bands in the blue protein RR spectra to be accounted for by metal–ligand stretches, and attention must turn to other vibrational modes that might be enhanced. The most plausible candidates are internal modes of the metal-bound ligands, which might gain intensity either directly, through involvement in the excited-state distortion, or indirectly via (ground-state) vibrational coupling with the metal–ligand stretches. Since the resonant electronic transition is associated with (Cys) → Cu charge transfer (Gray & Solomon, 1981), attention naturally focuses on the cysteine modes. A diagram of the Cu–Cys fragment is shown in Figure 9. In addition to the Cu–S(Cys) stretch, modes that should directly modulate the electronic transition by shifting the energies of the S orbitals include the C–S stretch and the Cu–S–C bend. The C–S stretch, assigned at ∼750 cm^{-1} (Ferris et al., 1979), does show modest enhancement (Figure 3). Since angle-bending modes are generally found at about half the mean stretching frequency of the bonds forming the angle, the Cu–S–C bend is expected to be near 290 cm^{-1}. A plausible assignment would be to one component of the composite band at ∼265 cm^{-1}, the other being the symmetric Cu–N(His) stretch, as discussed above. Alternatively, a weak band seen at 333 cm^{-1} in laccase and stellacyanin might arise from this mode.

A particularly important coordinate is the $\delta_{SC_\alpha C_\beta}$ angle bend, whose natural frequency is in the 300–400 cm^{-1} range and

which can interact strongly with the adjacent Cu–S bond. The interaction is sensitive to the τ_{CuSCC} dihedral angle, being maximal at $\tau = 180°$ (trans conformation, illustrated in Figure 9) when the Cu–S stretching and SCC bending coordinates are in line and minimal at $\tau = 90°$. The situation is analogous to that found in disulfides (Sugeta, 1975), the S–S stretching frequency, at ~520 cm^{-1}, being sensitive to the τ_{SSCC} dihedral angle. The interaction should be much stronger for Cu–S stretching because of the closer frequency match of the two coordinates. Model normal-mode calculations for the Fe(Cys)$_4$ protein rubredoxin (Yachandra et al., 1983) show that the δ_{SCC} bend is an important determinant of the Fe–S stretching frequencies, which vary with the dihedral angle. Strong mixing of Cu–S stretching and SCC bending may account for the pair of prominent stellacyanin bands, 347 and 385 cm^{-1}, each of which show half the ^{63}Cu/^{65}Cu isotope shift expected for the Cu–S stretching mode by itself. The situation in laccase, however, is more complicated, since the 381- and 405-cm^{-1} bands each show only ~20% of the expected Cu–S shift and there is a third intense band, 420 cm^{-1}, whose shift is even smaller.

In addition to δ_{SCC}, there are three other cysteine angle bend coordinates with natural frequencies in the 300–500-cm^{-1} range: $\delta_{C_\beta C_\alpha(CO)}$, $\delta_{C_\beta C_\alpha N}$, and $\delta_{NC_\alpha(CO)}$. However, these angles are separated from the Cu–S bonds by one or more intervening bonds, and it is not at all evident that vibrational mixing with the Cu–S stretch can be substantial or, alternatively, that a mechanism exists for involving these coordinates directly in the excited-state distortion. The same reservations apply, with greater force, to bending coordinates that are further removed, along the polypeptide chain. The remaining cysteine internal coordinates involve C–C stretching or C–H bending, which are expected at much higher frequencies, in the 900-cm^{-1} region, or torsions about the single bonds, which are normally at much lower frequencies.

It is conceivable, however, that these torsional motions are raised substantially in frequency by the anchoring of the atoms in the protein structure. The τ_{CuSCC} mode, for example, is more akin to a chelate puckering mode than to the torsional mode of a monodentate thiolate ligand. Such a mode might be directly linked to the S → Cu charge-transfer transition because of its effect on the orientations of the sulfur orbitals and their overlap with the Cu orbitals. Whether its frequency can plausibly be expected to be as high as ~400 cm^{-1} is uncertain; no model systems have been analyzed from this point of view. It may be relevant, however, that the o-xylene-α,α'-dithiolato chelate Fe(S$_2$-o-xyl)$^-$ has been shown to have ligand modes in the 300–500-cm^{-1} region that are sensitive to deuteration at the methylene positions and that interact significantly with the Fe–S stretching modes (Yachandra et al., 1983).

The other blue-site ligands, Met and His, also have bending modes in the 400-cm^{-1} region. These seem to us less likely as candidates for resonance enhancement because of the minimal involvement of these ligands in the resonant electronic transition. There is precedent, in the case of oxyhemocyanin (Larrabee et al., 1977; Larrabee & Spiro, 1980), for strong enhancement of Cu–N(His) stretching modes via resonance with a charge-transfer transition from another ligand (O$_2^{2-}$ → Cu^{II}), but for the blue proteins the Cu–N(His) stretch, identified at ~265 cm^{-1}, is enhanced only modestly. It seems unlikely that internal histidine modes would gain very much intensity via vibrational mixing with Cu–N(His) stretching or via direct involvement in the electronic transition. They may, however, contribute to some of the weaker RR bands, as Woodruff et al. (1983a,b) have emphasized. The imidazole

ring has no in-plane deformation modes below 700 cm^{-1} (Colombo et al., 1974; Cordes & Walter, 1968). It does have a pair of out-of-plane ring deformation modes, which fall in the 400–600-cm^{-1} region (Colthup, 1964); these are expected to shift significantly in D$_2$O, because of coupling with the N–H(D) out-of-plane bend. It is possible that the D$_2$O-sensitive stellacyanin RR shoulders at 359 and 374 cm^{-1} are ImH out-of-plane bends, although the frequencies are somewhat low. (Another possibility is that they involve motion of the cysteine peptide N, whose proton may have been exchanged in D$_2$O.) Histidine also has modes involving the C$_\alpha$ and C$_\beta$ atoms, which may be in the right frequency range, but these are quite distant from the chromophore.

Since the methionine does not appear to be involved in the electronic transition or to give an identifiable Cu–S(Met) stretch (except, perhaps, in azurin at low temperature; Woodruff et al., 1983b), its internal modes also seem unlikely candidates for resonance enhancement.

Conclusions

The isotope shifts and normal-coordinate calculations described in the preceding sections make it clear that the RR spectra of blue copper sites are *not* dominated by metal–ligand stretching modes. One component of the moderate intensity band at ~265 cm^{-1} is assigned to Cu–N(His) stretching, but none of the strong bands near 400 cm^{-1} can be so assigned. Contributions from Cu–S(Met) stretching, if any, are expected at low frequencies. Only Cu–S(Cys) stretching can be significantly involved in the ~400-cm^{-1} bands, and the ^{63}Cu/^{65}Cu shifts in stellacyanin and laccase indicate that this coordinate contributes only 50% or less to any of the strong bands.

Internal modes of the Cu ligands must therefore be major contributors to the Raman scattering. A likely candidate is the SCC bend of the cysteine side chain, which can couple strongly with the Cu–S stretch. This coupling might account for the pair of strong stellacyanin RR bands, since each of them show half the ^{63}Cu/^{65}Cu shift expected for Cu–S(Cys) stretching. Additional couplings are implicated for laccase, however, whose strong bands show substantially smaller ^{63}Cu/^{65}Cu shifts. Thus, the normal-mode compositions are quite different for stellacyanin and laccase, probably reflecting different conformations of the protein ligands.

The large number of blue-site RR bands remains perplexing and requires further study. It is difficult to understand how numerous angle-bending coordinates, of the kind that normally would fall in the 300–500-cm^{-1} region, can be involved in resonance enhancement. A possibility that merits further consideration is that restricted torsional motions of the cysteine S–C bond might be involved in some of the modes.

References

Adman, E. T., & Jensen, L. H. (1981) *Isr. J. Chem. 21*, 8.

Adman, E. T., Stenkamp, R. E., Sicker, L. R., & Jensen, L. H. (1978) *J. Mol. Biol. 123*, 35.

Avery, J. S., Burbridge, C. D., & Goodgame, D. M. L. (1968) *Spectrochim. Acta, Part A 24A*, 1721.

Blair, D. F., Campbell, G. W., Lum, V., Martin, C. T., Gray, H. B., Malmström, B. G., & Chan, S. I. (1983) *J. Inorg. Biochem. 19*, 65.

Boden, N., Holmes, M. C., & Knowles, P. F. (1974) *Biochem. Biophys. Res. Commun. 57*, 845.

Colman, P. M., Freeman, H. C., Guss, J. M., Murata, M., Norris, V. A., Ramshaw, J. A. M., & Venkatappa, M. P.

(1978) *Nature (London)* 272, 319.

Colombo, L., Blackman, P., Schrader, B., Schneider, R., & Plesser, T. (1974) *J. Chem. Phys.* 61, 3270.

Colthup, B. C., Daly, L. H., & Wilberley, S. E. (1964) *Introduction to Infrared and Raman Spectroscopy*, 3rd ed., pp 236–237, Academic Press, New York.

Cordes, M., & Walter, J. L. (1968) *Spectrochim. Acta, Part A 24A*, 237.

Fahraeus, G. & Reinhammar, B. (1967) *Acta Chem. Scand.* 21, 2367.

Fawcett, T. G., Bernaducci, E. E., Krogh-Jespersen, K., & Schugar, H. J. (1980) *J. Am. Chem. Soc.* 102, 2598.

Fee, J. A. (1975) *Struct. Bonding (Berlin)* 23, 1.

Ferris, N. S., Woodruff, W. H., Rorabacher, D. B., Jones, T. E., & Ochrymowycz, L. A. (1978) *J. Am. Chem. Soc.* 100, 5939.

Ferris, N. S., Woodruff, W. H., Tennent, D. L., & McMillin, D. R. (1979) *Biochem. Biophys. Res. Commun.* 88, 288.

Freeman, H. C. (1980) *Coord. Chem.* 21, 29.

Freeman, H. C., & Solomon, E. I. (1981) *J. Am. Chem. Soc.* 103, 4382.

Glick, M. D., Gavel, D. P., Diaddario, L. L., & Rorabacher, D. B. (1976) *Inorg. Chem.* 15, 1190.

Goodgame, D. M. L., Goodgame, M., Hayward, P. J., & Rayner-Canham, G. W. (1968) *Inorg. Chem.* 7, 2447.

Gray, H. B., & Solomon, E. I. (1981) *Met. Ions Biol.* 3, 1.

Grazani, M. T., Morpurgo, L., Rotilio, G., & Mondovi, B. (1976) *FEBS Lett.* 70, 87.

Hauenstein, B. L., & McMillan, D. R. (1978) *Biochem. Biophys. Res. Commun.* 85, 505.

Herschbach, D. R., & Laurie, V. W. (1961) *J. Chem. Phys.* 35, 458.

Hill, H. A. O., Leer, J. C., Smith, B. E., Storm, C. B., & Ambler, R. P. (1976) *Biochem. Biophys. Res. Commun.* 70, 331.

Johnson, M. K., & Czernuszewicz, R. S. (1983) *Appl. Spectrosc.* 37, 297.

Laane, J., & Kiefer, W. (1980) *J. Chem. Phys.* 72, 5305.

Larrabee, J. A., & Spiro, T. G. (1979) *Biochem. Biophys. Res. Commun.* 88, 753.

Larrabee, J. A., & Spiro, T. G. (1980) *J. Am. Chem. Soc.* 102, 4217.

Larrabee, J. A., Spiro, T. G., Ferris, N. S., Woodruff, W. H., Maltese, W. A., & Kerr, M. S. (1977) *J. Am. Chem. Soc.* 99, 1979.

LuBien, C. D., Winkler, M. E., Thamann, T. J., Scott, R. A., Co, M. S., Hodgson, K. O., & Solomon, E. I. (1981) *J. Am. Chem. Soc.* 103, 7014.

Malkin, R., & Malmström, B. G. (1970) *Adv. Enzymol. Relat. Areas Mol. Biol.* 33, 177.

Malkin, R., Malmström, B. G., & Vänngard, T. E. (1969) *J. Biochem. (Tokyo)* 7, 253.

Markley, J. L. (1975) *Acc. Chem. Res.* 8, 70.

Markley, J. L., Ulrich, E. L., Berg, S. P., & Krogmann, D. W. (1975) *Biochemistry* 14, 4428.

McFadden, D. L., McPhail, A. T., Gardner, C. D., & Mablos, F. E. (1976) *J. Chem. Soc., Dalton Trans.*, 47.

McMillin, D. R., Holwerda, R. A., & Gray, H. B. (1974a) *Proc. Natl. Acad. Sci. U.S.A.* 71, 1338.

McMillin, D. R., Rosenberg, R. C., & Gray, H. B. (1974b) *Proc. Natl. Acad. Sci. U.S.A.* 71, 4428.

Mims, W. B., & Peisach, J. (1978) *J. Chem. Phys.* 69, 4921.

Mims, W. B., & Peisach, J. (1979) *J. Biol. Chem.* 254, 4321.

Miskowski, V. M., Tang, S.-P. W., Spiro, T. G., Shapiro, E., & Moss, T. H. (1975) *Biochemistry* 14, 1244.

Morpurgo, L., Finazzi-Agro, A., Rotilio, G., & Mondovi, B. (1972) *Biochim. Biophys. Acta* 205, 292.

Nakamoto, K. (1978) *Infrared and Raman Spectroscopy of Inorganic and Coordination Compounds*, 3rd ed., pp 212–213, Wiley, New York.

Parker, G. D. (1964) *Mellor's Inorganic Chemistry*, pp 653–654, Longmans, New York.

Peisach, J., Levine, W. G., & Blumberg, W. E. (1967) *J. Biol. Chem.* 242, 2847.

Peisach, J., Powers, L., Blumberg, W. E., & Chance, B. (1982) *Biophys. J.* 38, 277.

Penfield, K. W., Gay, R. R., Himmelwright, R. S., Eickman, N. C., Norris, V. A., Freeman, H. C. & Solomon, E. I. (1981) *J. Am. Chem. Soc.* 103, 4382.

Reinhammar, B. (1970) *Biochim. Biophys. Acta* 205, 35.

Reinhammar, B. (1983) *J. Inorg. Biochem.* 18, 113.

Reinhammar, B., & Oda, Y. (1979) *J. Inorg. Biochem.* 11, 115.

Reinhammar, B., & Malmström, B. G. (1981) *Met. Ions. Biol.* 3, 131.

Rist, G. H., Hyde, J. S., & Vänngard, T. (1970) *Proc. Natl. Acad. Sci. U.S.A.* 67, 79.

Roberts, J. E., Brown, T. G., Hoffman, B. M., & Peisach, J. (1980) *J. Am. Chem. Soc.* 102, 825.

Rousseau, D. L. (1981) *J. Raman Spectrosc.* 10, 94.

Salama, S., & Spiro, T. G. (1978) *J. Am. Chem. Soc.* 100, 1105.

Santoro, A., Mitchell, A. D., Zocchi, M., & Reimann, C. W. (1969) *Acta Crystallogr., Sect. B B25*, 842.

Scott, D. W., & El-Sabban, M. Z. (1969) *J. Mol. Spectrosc.* 30, 317.

Scott, R. A., Hahn, J. E., Doniach, S., Freeman, H. C., & Hodgson, K. O. (1982) *J. Am. Chem. Soc.* 104, 5364.

Shelnutt, J. A., Rousseau, D. L., Friedman, J. M., & Simon, S. R. (1979) *Proc. Natl. Acad. Sci. U.S.A.* 76, 409.

Shimanouchi, T., Nakagawa, I., Hiraishi, J., & Ishii, M. (1966) *J. Mol. Spectrosc.* 19, 78.

Siiman, O., & Carey, P. R. (1980) *J. Inorg. Biochem.* 12, 353.

Siiman, O., Young, N. M., & Carey, P. R. (1974) *J. Am. Chem. Soc.* 96, 5583.

Siiman, O., Young, N. M., & Carey, P. R. (1976) *J. Am. Chem. Soc.* 98, 744.

Solomon, E. I., Hare, J. W., & Gray, H. B. (1976a) *Proc. Natl. Acad. Sci. U.S.A.* 73, 1389.

Solomon, E. I., Rawlings, J., McMillin, D. R., Stephens, P. J., & Gray, H. B. (1976b) *J. Am. Chem. Soc.* 98, 8046.

Solomon, E. I., Hare, J. W., Dooley, D. M. Dawson, J. H., Stephens, P. J., & Gray, H. B. (1980) *J. Am. Chem. Soc.* 102, 168.

Spiro, T. G., & Stein, P. (1977) *Annu. Rev. Phys. Chem.* 28, 501.

Sugeta, H. (1975) *Spectrochim. Acta, Part A 31A*, 1729.

Thamann, T. J., Frank, P., Willis, L. J., & Loehr, T. M. (1982) *Proc. Natl. Acad. Sci. U.S.A.* 79, 6396.

Tosi, L., Garnier, A., Herve, M., & Steinbuch, M. (1975) *Biochem. Biophys. Res. Commun.* 65, 100.

Tullius, T. D., Frank, P., & Hodgson, K. O. (1978) *Proc. Natl. Acad. Sci. U.S.A.* 75, 4069.

Ugerbil, K., Norton, R. S., Allerhand, A., & Bersohn, R. (1977) *Biochemistry* 16, 886.

Vänngard, T. (1972) in *Biological Applications in Electronspin Resonance* (Swartz, H., Bolton, J. R., & Borg, D. C., Eds.) pp 411–447, Wiley-Interscience, New York.

Walters, M. A., & Spiro, T. G. (1983) *Inorg. Chem.* (in press).

Woodruff, W. H., Norton, K. A., Swanson, B. I., & Fry, H. A. (1983a) *J. Am. Chem. Soc. 105*, 657.

Woodruff, W. H., Norton, K. A., Swanson, B. I., & Fry, H. A. (1983b) *Proc. Natl. Acad. Sci. U.S.A.* (in press).

Woodruff, W. H., Norton, K. A., Swanson, B. I., Fry, H. A.,

& Malmström, B. G. (1983c) *Inorg. Chim. Acta 79*, 51.

Wright, P. G., Stein, P., Burke, J. M., & Spiro, T. G. (1979) *J. Am. Chem. Soc. 101*, 3531.

Yachandra, V. K., Hare, J., Moura, I., & Spiro, T. G. (1983) *J. Am. Chem. Soc.* (in press).

Zaslaw, B., & Rundle, R. E. (1961) *J. Phys. Chem. 57*, 490.

A Thermodynamic Model of the Lamellar to Inverse Hexagonal Phase Transition of Lipid Membrane–Water Systems[†]

Gregory L. Kirk, Sol M. Gruner,* and D. L. Stein

ABSTRACT: A theoretical model of the lamellar (L_α) to inverted hexagonal (H_{II}) phase transition is developed for mixtures of water and biological lipids. A free energy per lipid molecule is calculated for each phase as the sum of four lattice-specific terms: a local elastic term and global terms involving the packing of hydrocarbon chains, Debye-shielded electrostatics, and hydration effects. A critical lipid concentration for the transition is indicated by the concentration where the net lamellar and hexagonal free energies are equal. The relevance of the model to membrane interactions in biological systems is discussed. Suggestions are made for introducing temperature dependence into the model, and experiments are proposed to investigate the principal opposing forces in the model.

$\mathbf{I}$t is important to understand the microscopic factors governing the lamellar (L_α)[1] to inverted hexagonal (H_{II}) (Deamer et al., 1970) phase transition in biological lipids. The foremost physiological role of phospholipid is the formation of the bilayer membranes that compartmentalize cellular functions. Certain commonly encountered lipids (e.g., PE and CL) can convert to a nonbilayer phase inimical to compartmentalization, suggesting careful regulation of this transition by living cells. The L_α to H_{II} transition has been investigated experimentally by determining the phase diagrams of bulk lipid extracts vs. water concentration and temperature [see Luzzati (1968) for a review].

A major difficulty is in understanding how the experimental results on bulk systems apply to living cells. For example, it is known that bulk PE–water mixtures undergo a lamellar to H_{II} transition at physiological temperatures as the water concentration is decreased (Reiss-Husson, 1967). It is often argued that these conditions bear little relevance to living cells because cells always contain much water. This argument is misleading in that it ignores the range and nature of the microscopic forces driving the phase transition and the diversity of microenvironments encountered in cells. To illustrate, consider a comparison of the local conditions in two situations. In the first, consider the free energy of a lipid molecule in a bulk lamellar lipid–water mixture, undergoing the lamellar to H_{II} phase transition. In the second, consider the free energy of the lipid molecule in the near-contact zone between two closely opposed membrane vesicles, as in vesicle fusion. In either case, the lipid molecule in a bilayer environment faces a thin aqueous layer and is subject to the strong short-range (<50-Å) forces present between membrane surfaces.

In this paper, it is shown that the net free energy rises steeply as the thickness of the intervening aqueous space between the bilayers decreases. The free energy rises less steeply for a local cluster of inverted lipid tubes with the same succession of lipid

to water ratios. At some point, the free energies cross, and it becomes energetically favorable for the lipid to be in the inverted cylinder geometry. Locally, the situation is similar in both the bulk lipid and the approaching vesicle cases. It is in this local sense that one may use the experimental data on isolated bulk systems and consider the applicability of the model to cells.

We assume that the minimum free energy of a given number of lipid and water molecules is dominated by four geometry-dependent forces: lipid monolayer elasticity (curvature), electrostatics, hydrocarbon chain packing, and a surface hydration force. Three specific geometries are considered: lamellar, H_{II}, and close-packed inverted spherical micelles. In each case, a free energy associated with each of the four interactions is computed at a given lipid to water ratio. The geometry with the lowest total free energy is taken as the energetically favored phase at that concentration. This is used to predict the sequence of the three phases that would be observed in a bulk lipid–water system in equilibrium as a function of concentration. We consider three geometries consistent with the constraints of the hydrophobic effect. Rigorously, one would have to apply the approach to all possible geometries to predict the equilibrium state. In bulk lipid systems, lamellar and H_{II} phases *do* occur; consequently, it is logical, and computationally tractable, to apply the approach to them. In cells, the boundary conditions are more complex and more geometries must be considered. The important point is that, given a pair of geometries, this approach may be used to determine which of the two is favored in equilibrium. Cellular systems are additionally complicated by the effects of other components (e.g., proteins) and nonequilibrium behavior. Because the approach specifies a well-defined local free energy, it may be used in cases where no distinct lattice exists. Examples are intermembrane particles (deKriujff et al., 1979), tight junctions (Pinto da Silva,

[1] Abbreviations: L_α, lamellar; H_{II}, inverse hexagonal; C_{II}, inverse cubic; PE, phosphatidylethanolamine; PC, phosphatidylcholine; CL, cardiolipin; PS, phosphatidylserine; Ca^{2+}, calcium ion; T_c, gel to liquid-crystalline transition temperature.